

# Investigating the dark matter minispikes with the gamma-ray signal from the halo of M31

Zi-Qing Xia<sup>a1</sup>, Zhao-Qiang Shen<sup>a2</sup>, Xu Pan<sup>a,b</sup>, Lei Feng<sup>a,b,c3</sup>,  
Yi-Zhong Fan<sup>a,b</sup>

<sup>a</sup>Key Laboratory of DM and Space Astronomy, Purple Mountain Observatory, Chinese Academy of Sciences, Nanjing 210033, China

<sup>b</sup>School of Astronomy and Space Science, University of Science and Technology of China, Hefei, Anhui 230026, China

<sup>c</sup>Joint Center for Particle, Nuclear Physics and Cosmology, Nanjing University – Purple Mountain Observatory, Nanjing 210093, China

E-mail: [xiazq@pmo.ac.cn](mailto:xiazq@pmo.ac.cn), [zqshen@pmo.ac.cn](mailto:zqshen@pmo.ac.cn), [xupan@pmo.ac.cn](mailto:xupan@pmo.ac.cn),  
[fenglei@pmo.ac.cn](mailto:fenglei@pmo.ac.cn), [yzfan@pmo.ac.cn](mailto:yzfan@pmo.ac.cn)

**Abstract.** Recently, the evidence for gamma-ray emission has been found in the *Fermi*-LAT observation for the outer halo of Andromeda galaxy (M31). The dark matter (DM) annihilation offers a possible explanation on the gamma-ray radiation. In this work, we focus on the dark matter annihilation within minispikes around intermediate-mass black holes (IMBHs) with masses ranging from  $100 M_{\odot}$  to  $10^6 M_{\odot}$ . When the thermal annihilation relic cross section  $\langle\sigma v\rangle = 3 \times 10^{-26} \text{ cm}^3 \text{ s}^{-1}$  is adopted, we conduct an investigation on the population of IMBHs in the spherical halo area of M31. We find that there could be more than 65 IMBHs with masses of  $100 M_{\odot}$  surrounded by the DM minispikes as the remnants of Population III stars in the M31 spherical halo, and it is almost impossible for the existence of minispikes around IMBHs with masses above  $10^4 M_{\odot}$  which could be formed by the collapse of primordial cold gas, for both dark matter annihilation channels  $b\bar{b}$  and  $\tau^+\tau^-$ . The properties of dark matter have been further explored with the simulation of these two scenarios for IMBHs formation.

---

<sup>1</sup>Corresponding author.

<sup>2</sup>Corresponding author.

<sup>3</sup>Corresponding author.

---

## Contents

<b>1</b>	<b>Introduction</b>	<b>1</b>
<b>2</b>	<b>Dark matter model</b>	<b>2</b>
2.1	Gamma-rays from DM annihilation	2
2.2	DM density distribution	3
2.3	IMBHs formed in the early universe	3
<b>3</b>	<b>Limit on the population of IMBHs</b>	<b>4</b>
3.1	Data and analysis	4
3.2	Result	5
<b>4</b>	<b>Discussion</b>	<b>6</b>
<b>5</b>	<b>Summary</b>	<b>7</b>

---

## 1 Introduction

Dark matter (DM) is proposed to explain the missing mass which makes up approximately 85% of the matter in the current universe. There are a large number of astrophysical observations establishing the presence of DM [1, 2]. But the nature of DM is still far from clear. Among many hypothetical particle models, Weakly Interacting Massive Particles (WIMPs) are perceived as one of the most promising DM candidates [3–6]. WIMPs could annihilate into standard model particles which can further produce gamma rays and cosmic rays. The present-day energy density of DM reveals that the cross section of WIMPs annihilation averaged over the velocity distribution through the s-wave process is about  $\langle\sigma v\rangle = 3 \times 10^{-26} \text{ cm}^3 \text{ s}^{-1}$ , called as the thermal relic cross section [7]. The end products of WIMPs annihilation could be observed by the astronomical telescopes, which provides a feasible way to search for DM indirectly.

The observations of the gamma-ray sky have been widely used to indirectly detect DM [8]. The dwarf spherical galaxies [9–15] and the Galactic center [16–22] are prevailing targets for WIMPs searches. Especially for the dwarf galaxies, due to the high mass-to-light ratio, their observations have set the most stringent limits on WIMPs [11]. Nearby galaxies are also regarded as interesting targets [23–29]. M31 is the nearest large galaxies, its gamma-ray emission was first detected by the Fermi Large Area Telescope (*Fermi*-LAT) in Ref. [23], and the corresponding DM constraints were then presented in Ref. [25]. Ref. [28] has found that with the smooth DM spatial distribution, signals of DM particle interactions were insufficient to explain all the gamma-ray emission from M31 which was detected with the  $0.4^\circ$  extension.

Interestingly, Ref. [29] separated M31 into three spherically symmetric components centered at the M31 (i.e. the inner galaxy, spherical halo and far outer halo) and reported a gamma-ray excess toward the halo region of M31. The DM origin of the gamma-ray signal from the M31 spherical halo (M31SH) have been studied in Ref. [30, 31]. Tab. II in Ref. [30] has shown that in the case of the smooth Navarro-Frenk-White (NFW) density distribution

in M31SH, the best-fit DM annihilation cross section  $\langle\sigma v\rangle = 787 \times 10^{-26} \text{ cm}^3 \text{ s}^{-1}$  (with the best-fit DM mass  $m_\chi = 50 \text{ GeV}$ ) is obviously far above the thermal relic cross section  $\langle\sigma v\rangle = 3 \times 10^{-26} \text{ cm}^3 \text{ s}^{-1}$  and has been excluded by the limits from the dwarf spherical galaxies observation. Except for the annihilation cross section, the gamma-ray flux from the DM annihilation is also proportional to the square of the DM density. It implies that with the thermal relic cross section, enhancements of the DM density (compared with the smooth NFW profile) are needed to yield the measured high gamma-ray flux toward the M31SH. Substructures (or called subhalos) in the DM halos of both M31 and the Milky Way have been introduced to explain this issue in Ref. [30, 31].

In this paper, we propose another scheme to enhance the DM density in M31SH by using the minispikes around intermediate-mass black holes (IMBHs). IMBHs from  $100 M_\odot$  to  $10^6 M_\odot$  are supposed to be the generic prediction of supermassive black holes and could originate from the collapses of Population III (Pop. III) stars or primordial cold gas in the early universe [32, 33]. Some of the ultraluminous X-ray sources are thought to be the IMBH candidates [34, 35]. If the IMBHs exist in the M31SH region, due to their adiabatic growth, the surrounding DM would form the minispikes structure with high densities [36]. Due to the limited spatial resolution of *Fermi*-LAT, the DM minispikes could contribute the gamma-ray excess of M31SH as the unresolved point sources, providing a possible explanation on the high flux from the M31SH. Since they were proposed, the minispikes around IMBHs have been widely studied for the DM indirect detection with the observations of the gamma-ray telescopes [36–47] and the neutrino telescope [48].

Here we will investigate on the population of IMBHs in M31SH using the observed gamma-ray spectrum in the framework of the DM self-annihilation. The paper is organized as follows: In Sec. 2, we present the DM model used to calculate the gamma-ray flux from WIMPs annihilation in M31SH and introduce two proposed scenarios for IMBHs formed in the early universe. In Sec. 3, we use the gamma-ray spectrum of M31SH to set limit on the population of IMBHs given the thermal relic cross section  $\langle\sigma v\rangle = 3 \times 10^{-26} \text{ cm}^3 \text{ s}^{-1}$ . In Sec. 4, the *Scenario PopIII* and *Scenario PCGas* of IMBHs are discussed in detail for the M31SH to constrain the property of WIMPs. Sec. 5 summarizes our results and discussions.

## 2 Dark matter model

### 2.1 Gamma-rays from DM annihilation

The WIMPs are expected to annihilate with each other and then produce gamma rays through many different annihilation channels (i.e.  $b\bar{b}$  or  $\tau^+\tau^-$ ). The prompt gamma-ray flux from the DM annihilation can be given as a function of photon energy  $E_\gamma$  [8, 28]

$$\frac{d\Phi}{dE_\gamma}(E_\gamma) = \frac{\langle\sigma v\rangle}{8\pi m_\chi^2} \frac{dN_\gamma}{dE_\gamma} \times J_{\text{factor}}, \quad (2.1)$$

where  $m_\chi$  denotes the rest mass of the DM particles,  $\frac{dN_\gamma}{dE_\gamma}$  represents the differential photon production for the annihilation of a DM particle pair and can be obtained from the PPPC 4 DM ID<sup>1</sup> [49],  $J_{\text{factor}}$  characterizes the spatial distribution of the DM and is the line-of-sight (l.o.s.) integral of the square of the DM density  $\rho^2(r)$ . The  $J_{\text{factor}}$  within the region of interest (ROI) in one DM halo can be expressed as

$$J_{\text{factor}} = \int_{\Delta\Omega} \int_{\text{l.o.s.}} \rho^2(\mathbf{r}(s)) ds d\Omega, \quad (2.2)$$

---

<sup>1</sup><http://www.marcocirelli.net/PPPC4DMID.html>

where  $\Delta\Omega$  is the solid angle of ROI,  $s$  is the distance along the line of sight and  $r$  is the radial distance from the center of the halo.

## 2.2 DM density distribution

The DM density distribution in the region of M31SH can be divided into two types in our work: the Navarro-Frenk-White (NFW) profile and the Minispike (mns) profile. The DM density in the main galactic halo of M31 is often approximated with a NFW profile [50, 51] represented by

$$\rho(r) = \frac{\rho_s}{(r/r_s)(1+r/r_s)^2}, \quad (2.3)$$

where  $\rho_s$  is the characteristic density and  $r_s$  is the scale radius. Here we take the values of  $\rho_s$  and  $r_s$  as  $0.418 \text{ GeV cm}^{-3}$  and  $16.5 \text{ kpc}$ , respectively [52].

The DM density around IMBHs could be locally and dramatically enhanced by the adiabatic growth of IMBHs, forming the minispikes [53]. Here a non-rotating black hole (BH) is considered, and the DM profile in such a minispike is given as follows [45]:

$$\rho(r) = \begin{cases} 0 & r \leq 2R_S \\ \rho_{\text{sat}} & 2R_S < r \leq R_{\text{sat}} \\ \rho_0 \left( \frac{r}{R_{\text{sp}}} \right)^{-\gamma_{\text{sp}}} & R_{\text{sat}} < r \leq R_{\text{sp}} \end{cases}, \quad (2.4)$$

where the Schwarzschild radius is represented by  $R_S = 2GM_{\text{BH}}/c^2 = 2.95 \text{ km} (M_{\text{BH}}/M_\odot)$ , the saturation radius is given as  $R_{\text{sat}} = R_{\text{sp}}(\rho_{\text{sat}}/\rho_0)^{-1/\gamma_{\text{sp}}}$  to ensure the continuity of density, and the radius of the spike is defined as the typical radius of the BH influence  $R_{\text{sp}} = GM_{\text{BH}}\sigma_*^{-2} = 0.0043 \text{ pc} (M_{\text{BH}}/M_\odot)(\sigma_*/\text{km s}^{-1})^{-2}$  [47, 54]. The parameters  $G$  and  $\sigma_*$  are the gravitational constant and the stellar velocity dispersion, separately. We adopt the  $M_{\text{BH}}\text{-}\sigma_*$  relation for IMBHs  $\log(M_{\text{BH}}/M_\odot) = 8.13 + 4.02 \log(\sigma_*/200 \text{ km s}^{-1})$  as given in Ref. [55]. Then, the saturation density  $\rho_{\text{sat}} = m_\chi/(\langle\sigma v\rangle t_{\text{BH}})$  relies on the DM mass  $m_\chi$ , the annihilation cross section  $\langle\sigma v\rangle$  and the age of BH  $t_{\text{BH}}$  [56]. Here we focus on the IMBHs formed in the early universe and adopt  $t_{\text{BH}} \approx 10^{10} \text{ yr}$ . All the mass inside the minispike  $M_{\text{sp}}$  is required to be of the order of the BH mass  $M_{\text{BH}}$ , approximately with  $\rho_0 \approx (3 - \gamma_{\text{sp}})M_{\text{BH}}/(4\pi R_{\text{sp}}^3)$  [45]. Considering the initial NFW distribution in minispikes, we adopt  $\gamma_{\text{sp}} = 7/3$  as the redistributed spike index [33, 37].

## 2.3 IMBHs formed in the early universe

Here we briefly introduce two different scenarios for IMBHs formed in the early universe. The first scenario of IMBHs is originating from the Pop. III (or “first”) stars collapsing, called *Scenario PopIII* [57–60]. The final fate of zero-metallicity Pop. III stars depends on their initial stellar masses. Pop. III stars with the initial masses of  $60 M_\odot - 140 M_\odot$  would collapse to black holes after the final explosion [60]. In the mass range from roughly  $140 M_\odot$  up to  $260 M_\odot$ , the Pop. III star would produce a pair-instability supernova, without leaving a remnant [58]. For the high mass Pop. III star larger than  $260 M_\odot$ , the collapse into black hole can directly occur without explosion [60]. From above, the collapse of Pop. III stars with the mass  $60 M_\odot \leq M_{\text{BH}} \leq 140 M_\odot$  and  $M_{\text{BH}} \geq 260 M_\odot$  could lead to the formation of IMBHs at  $\sim 100 M_\odot$  [33, 61]. The second scenario of IMBHs is formed directly by the collapse of Primordial Cold Gas at high redshift, called *Scenario PCGas* [62–64]. The protogalactic disk could be formed in the center of early-forming halo. Due to the gas

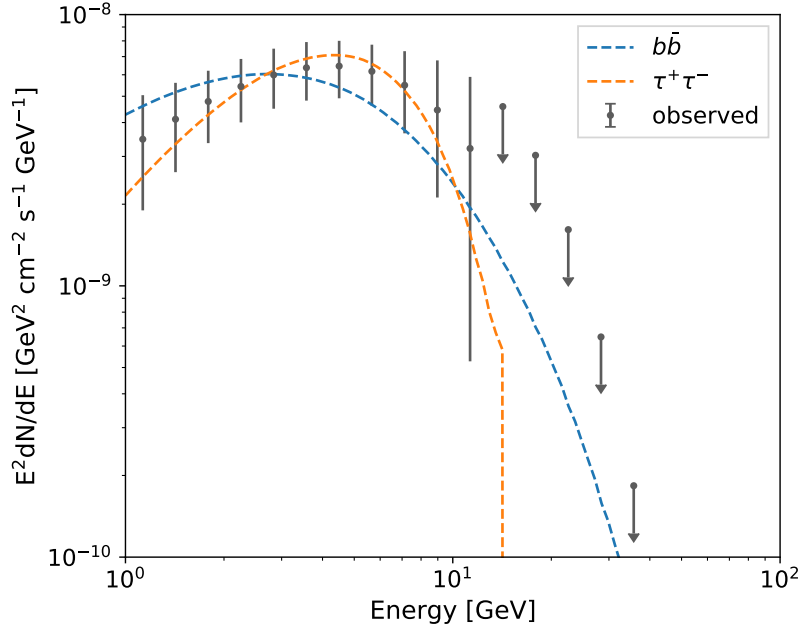


**Figure 1:** The energy spectrum of M31SH. The grey error bars represent the measured gamma-ray spectrum of M31SH in Ref. [29]. The blue (orange) dashed line is the best fit spectrum of DM annihilation we get with the  $b\bar{b}$  ( $\tau^+\tau^-$ ) channel.

cooling and the gravitational effect, the unstable disc could eventually collapse into an IMBH with a characteristic mass of  $\sim 10^5 M_\odot$  [64].

### 3 Limit on the population of IMBHs

#### 3.1 Data and analysis

The Large Area Telescope aboard the Fermi Space Telescope Mission (*Fermi*-LAT) is a current on-orbit high performance gamma-ray telescope for the photon energy range from 50 MeV to 1 TeV [65]. Using nearly 7.6 years of the *Fermi*-LAT observations, Ref. [29] has carefully studied the gamma-ray emission from the M31’s spherical halo with 20 evenly logarithmically spaced energy bins from 1 GeV to 100 GeV. The radial extension of the spherical halo ranges from  $0.4^\circ$  to  $8.5^\circ$  corresponding to a projected radius from 5.5 kpc to 117 kpc. Here we directly apply the best fit energy spectrum of M31SH from Ref. [29] to study the minispikes in M31, shown as the grey error bars in the Fig. 1.

We perform the *least square* method and the  $\chi^2$  analysis in the fit procedure. We notice that there are a few upper limits of flux in the spectrum of M31’s SH which are necessary to be taken into account in the fit. To consider upper limits, we define the  $\chi^2$  by two terms as [30, 66, 67]

$$\chi^2 = \chi_{\text{cl}}^2 + \chi_{\text{upl}}^2. \quad (3.1)$$

The first term on the left side  $\chi_{\text{cl}}^2$  is the classic  $\chi^2$  function for  $n$  measurements

$$\chi_{\text{cl}}^2 = \sum_i^n \left( \frac{f_i - \hat{f}_i(\theta)}{\sigma_i} \right)^2, \quad (3.2)$$

where  $f_i$ ,  $\sigma_i$  and  $\hat{f}_i(\theta)$  denote the measured flux, uncertainty and expected flux for the model parameters  $\theta$  in the  $i$ th energy bin, respectively. The second term  $\chi_{\text{upl}}^2$  quantifies the effect of  $m$  upper limits in our fit, defined by a set of the probability  $P$  with the expected flux  $\hat{f}_j$  smaller than the upper limit  $f_{\text{upl},j}$

$$\chi_{\text{upl}}^2 = -2\ln\left(\prod_j^m P(\hat{f}_j(\theta) < f_{\text{upl},j})\right) = -\sum_j^m 2\ln\left(\frac{1 + \text{erf}\left(\frac{f_{\text{upl},j} - \hat{f}_j(\theta)}{\sqrt{2}\sigma_j}\right)}{2}\right), \quad (3.3)$$

where the error function  $\text{erf}(x)$  is

$$\text{erf}(x) = \frac{2}{\sqrt{\pi}} \int_0^x e^{-t^2} dt. \quad (3.4)$$

For the observational spectrum of M31SH in Fig. 1, we have the number of measurements  $n = 11$ , the number of upper limits  $m = 9$  and the total  $n + m = 20$ .

### 3.2 Result

In this work, we plan to limit the population of IMBHs by using of the thermal relic cross section  $\langle\sigma v\rangle = 3 \times 10^{-26} \text{ cm}^3 \text{ s}^{-1}$  for s-wave. For simplicity, we assume IMBHs in the M31SH have the same mass of  $M_{\text{BH}}$ .

We fit the measured gamma-ray spectrum of M31SH in the Fig. 1 with the DM annihilation model in Eq. (2.1) with two DM annihilation channels  $b\bar{b}$  and  $\tau^+\tau^-$ , respectively. The DM mass  $m_\chi$  and the  $J_{\text{factor}}$  are set to be free in this fit process. We obtain that the best fit parameters for the  $b\bar{b}$  annihilation channel are  $m_\chi = 56.6 \text{ GeV}$  and

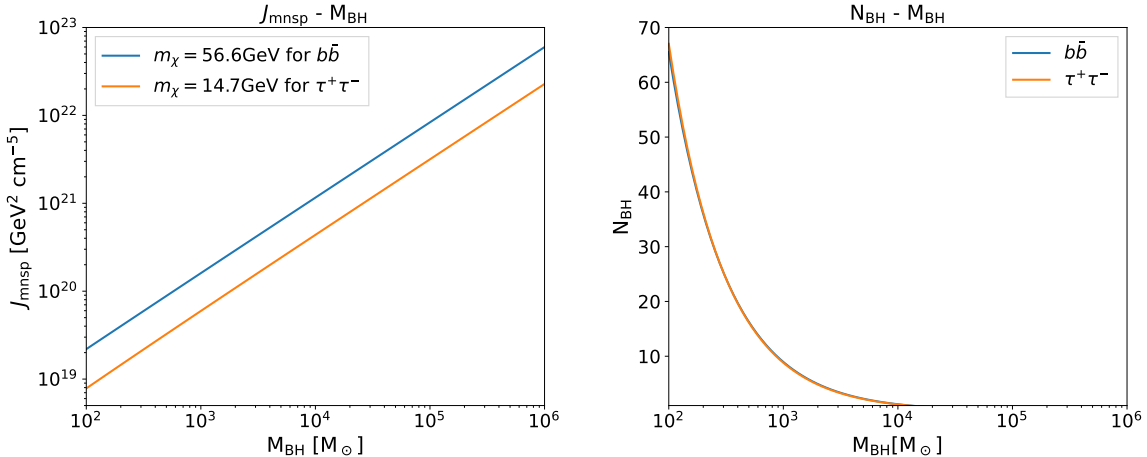


**Figure 2:** The left panel shows the relationship between the  $J_{\text{mnsp}}$  for DM minispike and the IMBHs mass  $M_{\text{BH}}$  given the best fit DM mass and the thermal relic cross section. The right panel shows limits on the number of IMBHs  $N_{\text{BH}}$  with the mass of  $M_{\text{BH}}$  in M31SH. For both panels, the blue and orange lines are on behalf of the  $b\bar{b}$  and  $\tau^+\tau^-$  channels, respectively.

$J_{\text{factor}} = 1.5 \times 10^{21} \text{ GeV}^2 \text{ cm}^{-5}$  ( $m_\chi = 14.7 \text{ GeV}$  and  $J_{\text{factor}} = 5.5 \times 10^{20} \text{ GeV}^2 \text{ cm}^{-5}$  for the  $\tau^+\tau^-$  channel). It is worth noting that the best fit DM mass for the  $b\bar{b}$  channel is very close to that of Ref. [68] ( $\sim 60 \text{ GeV}$ ) which can explain the muon  $g - 2$  measurement [69], the gamma-ray excess at the Galactic center [22] and the antiproton excess of AMS-02 [70, 71] together.

The  $J_{\text{factor}}$  for the M31SH field can be represented as the sum of the smooth NFW component and DM minispikes around IMBHs:

$$J_{\text{factor}} = J_{\text{NFW}} + N_{\text{BH}} \times J_{\text{minsp}}, \quad (3.5)$$

where  $J_{\text{NFW}} = 2.9 \times 10^{19} \text{ GeV}^2 \text{ cm}^{-5}$  is integrated within the area of M31SH ( $0.4^\circ - 8.5^\circ$ ), and the contribution from one DM minispoke  $J_{\text{minsp}}$  relies on the mass of IMBHs  $M_{\text{BH}}$ . When the best fit DM mass  $m_\chi$  and the thermal relic cross section  $\langle\sigma v\rangle = 3 \times 10^{-26} \text{ cm}^3 \text{ s}^{-1}$  is adopted, the relationships between the  $J_{\text{minsp}}$  and the IMBHs mass  $M_{\text{BH}}$  are given in the left panel of Fig. 2.

For a set of fixed IMBH mass  $M_{\text{BH}}$  from  $10^2 M_\odot$  to  $10^6 M_\odot$ , we can calculate the number of IMBHs in M31SH  $N_{\text{BH}}$  from the best fit  $J_{\text{factor}}$  obtained above. The results we get for different channels ( $b\bar{b}$  and  $\tau^+\tau^-$ ) are very close to each other as shown in the right panel of Fig. 2 and we find that the number of IMBHs with masses exceeding  $10^4 M_\odot$  surrounded by the DM minispikes is below one. In the Sec. 2.3, we note that the IMBHs from the *Scenario PopIII* have the masses of  $\sim 100 M_\odot$ , while the masses of the IMBHs in the *Scenario PCGas* are relatively large at  $\sim 10^5 M_\odot$ . It implies that more than 65 IMBHs with masses of  $100 M_\odot$  surrounded by the minispikes are expected to locate in the M31SH field as the remnants of Pop. III stars and rule out the existence of minispikes around IMBHs in the *Scenario PCGas* for both the  $b\bar{b}$  and  $\tau^+\tau^-$  channels.

## 4 Discussion

In the previous section, we use the standard assumption of thermal relic DM annihilation cross section to limit the population of IMBHs in M31SH. In this section, we discuss the *Scenario PopIII* and *Scenario PCGas* of IMBHs with the simulations to constrain the parameters of DM ( $m_\chi$  and  $\langle\sigma v\rangle$ ).

Ref. [33] has simulated the evolution of IMBHs in Milky Way galaxy starting from the early universe to the redshift  $z = 0$  and constructed 200 Monte-Carlo realizations of the IMBHs population in the halo of Milky Way for each scenario, respectively. The property of the IMBHs population in M31 is assumed to be similar to that in the Milky Way. We take the mass distribution of IMBHs in Ref. [33]. Considering the number of IMBHs is almost proportional to the virial mass of the host galactic halo, we rescale the number of IMBHs for M31 with the masses of Milky Way and M31 in Table I of the Ref. [37]. It is noticed that we only consider IMBHs in M31SH with the galactocentric distance from 5.5 kpc to 117 kpc. The radial distribution of IMBHs in M31 can be obtained by rescaling that of Milky Way in Fig.2 of the Ref. [33] with the virial radius of M31 180 kpc, and we find that almost 80% of IMBHs in M31 are located in M31SH for both scenarios.

In the case of *Scenario PopIII*, there are about  $N_{\text{BH}} = 558$  IMBHs in M31SH and the mass of IMBHs is given by the delta function of  $100 M_\odot$  [33]. The total  $J_{\text{factor}}$  in the M31SH field is given as the Eq. (3.5). While for the *Scenario PCGas*, we get that the number of IMBHs in M31SH is about  $N_{\text{BH}} = 52$  and the distribution of IMBHs mass is predicted to obey the *log - normal* distribution with the average mass  $M_{\text{BH}} = 10^5 M_\odot$  and a standard

**Table 1:** The best-fit DM parameters.

Annihilation Channel	Model	$m_\chi$ (GeV)	$\langle\sigma v\rangle$ ( $\text{cm}^3 \text{s}^{-1}$ )	Reduced $\chi^2$
$b\bar{b}$	<i>NFW</i>	$56.6 \pm 8.5$	$(1.25 \pm 0.26) \times 10^{-24}$	0.47
$b\bar{b}$	<i>Scenario PopIII</i>	$56.6 \pm 8.5$	$(1.56 \pm 0.48) \times 10^{-29}$	0.47
$b\bar{b}$	<i>Scenario PCGas</i>	$56.6 \pm 8.5$	$(1.46 \pm 0.35) \times 10^{-36}$	0.47
$\tau^+\tau^-$	<i>NFW</i>	$14.7 \pm 1.6$	$(5.75 \pm 0.81) \times 10^{-25}$	0.21
$\tau^+\tau^-$	<i>Scenario PopIII</i>	$14.7 \pm 1.6$	$(1.51 \pm 0.45) \times 10^{-29}$	0.21
$\tau^+\tau^-$	<i>Scenario PCGas</i>	$14.7 \pm 1.6$	$(1.18 \pm 0.31) \times 10^{-36}$	0.21

deviation  $\sigma_{BH} = 0.9$  as given in Ref. [33, 72]. Then we generate 300 Monte-Carlo realizations for 52 IMBHs masses in M31SH. For each realization, the total  $J_{\text{factor}}$  can be defined by

$$J_{\text{factor}} = J_{\text{NFW}} + \sum_i^{52} J_{\text{minsp}}(i), \quad (4.1)$$

where  $J_{\text{minsp}}(i)$  is the  $J_{\text{factor}}$  of the minispikes for the  $i$ th IMBH.

When  $J_{\text{factor}}$  prepared, we fit the spectrum of M31SH with the DM annihilation model in Eq. (2.1) using the same  $\chi^2$  method of the Sec. 3.1. The DM mass  $m_\chi$  and annihilation section  $\langle\sigma v\rangle$  are set to be free and the  $\chi^2$  can be described as a function of  $(m_\chi, \langle\sigma v\rangle)$ . The best-fit DM parameters for three models (*NFW*, *Scenario PopIII* and *Scenario PCGas*) are presented in Tab. 1. It is noted that we only take the  $J_{\text{NFW}}$  into account ( $J_{\text{factor}} = J_{\text{NFW}} = 2.9 \times 10^{19} \text{ GeV}^2 \text{ cm}^{-5}$ , with no minispikes in M31SH) for the *NFW* model. The best-fit DM parameters for the *NFW* model are in tension with current limits from searches of dwarf spheroidal galaxies. As with the *Scenario PCGas*, we perform the same analysis with for each realizations and take the average result of all 300 realizations. The  $\chi^2$  values with a series of  $(m_\chi, \langle\sigma v\rangle)$  are shown as colour maps in Fig. 3 of the Appendix.

The best fit annihilation cross sections  $\langle\sigma v\rangle$  for *Scenario PopIII* and *Scenario PCGas* are significantly less than  $3 \times 10^{-26} \text{ cm}^3 \text{ s}^{-1}$  which is the DM s-wave cross section yielding the correct relic density. It may indicate the possibility of the p-wave or d-wave DM annihilation where the cross sections rely on the velocity of DM particles ( $v$ ) [73]. If the velocity of DM particles in the minispikes around IMBHs is about several hundreds to several thousands kilometers per second, the current annihilation cross section  $\langle\sigma v\rangle$  for p-wave is  $\sim (v/c)^2 \sim 10^{-29} \text{ cm}^3 \text{ s}^{-1}$  and for d-wave is  $\sim (v/c)^4 \sim 10^{-36} \text{ cm}^3 \text{ s}^{-1}$ , which are exactly the best fit  $\langle\sigma v\rangle$  for *Scenario PopIII* and *Scenario PCGas* in Tab. 1, respectively.

Then we derive the exclusion on DM parameters. For a set of fixed DM masses  $m_\chi$  in the range 1 – 200 GeV, we calculate the  $\chi^2$  values in the Eq. (3.1) with the different annihilation cross sections  $\langle\sigma v\rangle$ . The 95% confidence level upper limit of  $\langle\sigma v\rangle$  is obtained when the  $\chi^2$  value is larger by 2.7 than the least value for each  $m_\chi$ . The upper limits of three models are represented as the black lines in the Fig. 3.

## 5 Summary

In this work, we investigate the DM explanation of gamma-ray excess from the M31SH region using the assumption of minispikes around IMBHs. First, we study the population of IMBHs in M31SH with the thermal relic cross section. We fit the M31SH’s spectrum data with the DM annihilation model. The best-fit  $J_{\text{factor}}$  of M31SH we obtain is larger than the

smooth NFW component  $J_{\text{NFW}}$ , which could be contributed by the DM minispikes around IMBHs located in the M31BH field. For the simplified assumption of IMBHs with the same mass, we infer the relationship between the number of IMBHs in M31SH  $N_{\text{BH}}$  and the IMBHs mass  $M_{\text{BH}}$  shown in the right panel of Fig. 2. For  $\sim 100 M_{\odot}$  IMBHs in the *Scenario PopIII*, we find that above 65 DM minispikes is needed to yield the observed spectrum of M31SH for both annihilation channels  $b\bar{b}$  and  $\tau^+\tau^-$ . And IMBHs with the masses above  $10^4 M_{\odot}$  in the *Scenario PCGas* surrounded by the DM minispikes can be excluded by the adoption of the thermal relic cross section.

However the nature of WIMPs is still unclear. Then we discuss the two different scenarios for IMBHs (*Scenario PopIII* and *Scenario PCGas*) with simulations to study the properties of DM. We rescale the IMBHs population of the Milky Way halo in the Ref. [33] for M31 and calculate the total  $J_{\text{factor}}$  of M31SH for each scenario individually. Then the spectrum of M31SH is refitted with the DM annihilation model to optimize the DM parameters ( $m_{\chi}$  and  $\langle\sigma v\rangle$ ). The best-fit DM masses and annihilation sections  $\langle\sigma v\rangle$  are listed in the Tab. 1 and the upper limits are derived in the Appendix.

## Acknowledgments

We thank Christopher M. Karwin for providing us with the spectrum data of M31SH, and Qiang Yuan, Yue-Lin Sming Tsai, Xiaoyuan Huang, Zhanfang Chen and Guan-Wen Yuan for valuable comments and discussions. We use the NumPy [74], SciPy [75], Matplotlib [76] and iminuit<sup>2</sup> packages in our analysis. This work is supported by the National Natural Science Foundation of China (No. U1738210, No. 12003069, No. 11773075, No. 12003074 and No. 12047560), the National Key Program for Research and Development (No. 2016YFA0400200) and the Entrepreneurship and Innovation Program of Jiangsu Province.

## References

- [1] W. Tucker, P. Blanco, S. Rappoport, L. David, D. Fabricant, E. E. Falco et al., *1E 0657-56: A Contender for the Hottest Known Cluster of Galaxies*, *Astrophys. J. Lett.* **496** (Mar., 1998) L5–L8, [[astro-ph/9801120](#)].
- [2] E. Corbelli and P. Salucci, *The extended rotation curve and the dark matter halo of M33*, *Mon. Not. R. Astron. Soc.* **311** (Jan., 2000) 441–447, [[astro-ph/9909252](#)].
- [3] G. Jungman, M. Kamionkowski and K. Griest, *Supersymmetric dark matter*, *Physics Reports* **267** (1996) 195–373.
- [4] G. Bertone, D. Hooper and J. Silk, *Particle dark matter: evidence, candidates and constraints*, *Phys. Rep.* **405** (Jan., 2005) 279–390, [[hep-ph/0404175](#)].
- [5] G. Bertone, D. Hooper and J. Silk, *Particle dark matter: evidence, candidates and constraints*, *Physics Reports* **405** (2005) 279–390.
- [6] J. L. Feng, *Dark matter candidates from particle physics and methods of detection*, *Annual Review of Astronomy and Astrophysics* **48** (2010) 495–545.
- [7] G. Steigman, B. Dasgupta and J. F. Beacom, *Precise relic wimp abundance and its impact on searches for dark matter annihilation*, *Phys. Rev. D* **86** (Jul, 2012) 023506.
- [8] E. Charles, M. Sánchez-Conde, B. Anderson, R. Caputo, A. Cuoco, M. Di Mauro et al., *Sensitivity projections for dark matter searches with the Fermi large area telescope*, *Phys. Rep.* **636** (June, 2016) 1–46, [[1605.02016](#)].

---

<sup>2</sup><https://github.com/scikit-hep/iminuit>

- [9] THE FERMI-LAT COLLABORATION collaboration, M. Ackermann, M. Ajello, A. Albert, W. B. Atwood, L. Baldini, J. Ballet et al., *Constraining dark matter models from a combined analysis of milky way satellites with the fermi large area telescope*, *Phys. Rev. Lett.* **107** (Dec, 2011) 241302.
- [10] FERMI-LAT COLLABORATION collaboration, M. Ackermann, A. Albert, B. Anderson, L. Baldini, J. Ballet, G. Barbiellini et al., *Dark matter constraints from observations of 25 milky way satellite galaxies with the fermi large area telescope*, *Phys. Rev. D* **89** (Feb, 2014) 042001.
- [11] THE FERMI-LAT COLLABORATION collaboration, M. Ackermann, A. Albert, B. Anderson, W. B. Atwood, L. Baldini, G. Barbiellini et al., *Searching for dark matter annihilation from milky way dwarf spheroidal galaxies with six years of fermi large area telescope data*, *Phys. Rev. Lett.* **115** (Nov, 2015) 231301.
- [12] D. Hooper and T. Linden, *On the gamma-ray emission from reticulum II and other dwarf galaxies*, *Journal of Cosmology and Astroparticle Physics* **2015** (sep, 2015) 016–016.
- [13] A. Geringer-Sameth, M. G. Walker, S. M. Koushiappas, S. E. Kopusov, V. Belokurov, G. Torrealba et al., *Indication of gamma-ray emission from the newly discovered dwarf galaxy reticulum ii*, *Phys. Rev. Lett.* **115** (Aug, 2015) 081101.
- [14] S. Li, Y.-F. Liang, K.-K. Duan, Z.-Q. Shen, X. Huang, X. Li et al., *Search for gamma-ray emission from eight dwarf spheroidal galaxy candidates discovered in year two of dark energy survey with fermi-lat data*, *Phys. Rev. D* **93** (Feb, 2016) 043518.
- [15] S. Li, K.-K. Duan, Y.-F. Liang, Z.-Q. Xia, Z.-Q. Shen, X. Li et al., *Search for gamma-ray emission from the nearby dwarf spheroidal galaxies with 9 years of fermi-lat data*, *Phys. Rev. D* **97** (Jun, 2018) 122001.
- [16] D. Hooper and L. Goodenough, *Dark matter annihilation in the galactic center as seen by the fermi gamma ray space telescope*, *Physics Letters B* **697** (2011) 412–428.
- [17] C. Gordon and O. Macías, *Dark matter and pulsar model constraints from galactic center fermi-lat gamma-ray observations*, *Phys. Rev. D* **88** (Oct, 2013) 083521.
- [18] B. Zhou, Y.-F. Liang, X. Huang, X. Li, Y.-Z. Fan, L. Feng et al., *GeV excess in the milky way: The role of diffuse galactic gamma-ray emission templates*, *Phys. Rev. D* **91** (Jun, 2015) 123010.
- [19] F. Calore, I. Cholis and C. Weniger, *Background model systematics for the fermi GeV excess*, *Journal of Cosmology and Astroparticle Physics* **2015** (mar, 2015) 038–038.
- [20] X. Huang, T. Enßlin and M. Selig, *Galactic dark matter search via phenomenological astrophysics modeling*, *Journal of Cosmology and Astroparticle Physics* **2016** (apr, 2016) 030–030.
- [21] M. Ajello, A. Albert, W. B. Atwood, G. Barbiellini, D. Bastieri, K. Bechtol et al., *Fermi-LAT Observations of High-Energy Gamma-Ray Emission toward the Galactic Center*, *Astrophysical Journal* **819** (Mar., 2016) 44, [1511.02938].
- [22] M. Ackermann, M. Ajello, A. Albert, W. B. Atwood, L. Baldini, J. Ballet et al., *The Fermi Galactic Center GeV Excess and Implications for Dark Matter*, *Astrophysical Journal* **840** (May, 2017) 43, [1704.03910].
- [23] A. A. Abdo, M. Ackermann, M. Ajello, A. Allafort, W. B. Atwood, L. Baldini et al., *Fermi Large Area Telescope observations of Local Group galaxies: detection of M 31 and search for M 33*, *Astron. Astrophys* **523** (Nov., 2010) L2, [1012.1952].
- [24] J. P. Lenain and R. Walter, *Search for high-energy  $\gamma$ -ray emission from galaxies of the Local Group with Fermi/LAT*, *Astron. Astrophys* **535** (Nov., 2011) A19, [1109.3321].

- [25] Z. Li, X. Huang, Q. Yuan and Y. Xu, *Constraints on the dark matter annihilation from Fermi-LAT observation of M31*, *J. Cosmol. Astropart. Phys.* **2016** (Dec., 2016) 028, [[1312.7609](#)].
- [26] M. Ackermann, M. Ajello, A. Albert, L. Baldini, J. Ballet, G. Barbiellini et al., *Observations of M31 and M33 with the Fermi Large Area Telescope: A Galactic Center Excess in Andromeda?*, *Astrophysical Journal* **836** (Feb., 2017) 208, [[1702.08602](#)].
- [27] L. Fu, Z. Q. Xia and Z. Q. Shen, *Search for the  $\gamma$ -ray emission from M33 with the Fermi Large Area Telescope*, *Mon. Not. R. Astron. Soc.* **471** (Oct., 2017) 1737–1742, [[1709.00131](#)].
- [28] M. Di Mauro, X. Hou, C. Eckner, G. Zaharijas and E. Charles, *Search for  $\gamma$ -ray emission from dark matter particle interactions from the Andromeda and Triangulum galaxies with the Fermi Large Area Telescope*, *Physical Review D* **99** (June, 2019) 123027, [[1904.10977](#)].
- [29] C. M. Karwin, S. Murgia, S. Campbell and I. V. Moskalenko, *Fermi-LAT Observations of  $\gamma$ -Ray Emission toward the Outer Halo of M31*, *Astrophysical Journal* **880** (Aug., 2019) 95, [[1812.02958](#)].
- [30] C. M. Karwin, S. Murgia, I. V. Moskalenko, S. P. Fillingham, A.-K. Burns and M. Fieg, *Dark matter interpretation of the Fermi-LAT observations toward the outer halo of M31*, *Physical Review D* **103** (Jan., 2021) 023027, [[2010.08563](#)].
- [31] A.-K. Burns, M. Fieg, A. Rajaraman and C. M. Karwin, *Dark matter explanations of the gamma-ray excesses from the Galactic Center and M31*, *Physical Review D* **103** (Mar., 2021) 063023, [[2010.11650](#)].
- [32] M. C. Miller and E. J. M. Colbert, *Intermediate-Mass Black Holes*, *International Journal of Modern Physics D* **13** (Jan., 2004) 1–64, [[astro-ph/0308402](#)].
- [33] G. Bertone, A. R. Zentner and J. Silk, *New signature of dark matter annihilations: Gamma rays from intermediate-mass black holes*, *Physical Review D* **72** (Nov., 2005) 103517, [[astro-ph/0509565](#)].
- [34] D. A. Swartz, K. K. Ghosh, A. F. Tennant and K. Wu, *The Ultraluminous X-Ray Source Population from the Chandra Archive of Galaxies*, *Astrophys. J. Suppl.* **154** (Oct., 2004) 519–539, [[astro-ph/0405498](#)].
- [35] D. R. Pasham, T. E. Strohmayer and R. F. Mushotzky, *A 400-solar-mass black hole in the galaxy M82*, *Nature* **513** (Sept., 2014) 74–76, [[1501.03180](#)].
- [36] H. Zhao and J. Silk, *Dark Minihalos with Intermediate Mass Black Holes*, *Physical Review Letters* **95** (June, 2005) 011301, [[astro-ph/0501625](#)].
- [37] M. Fornasa, M. Taoso and G. Bertone, *Gamma rays from dark matter minispikes in the Andromeda Galaxy M31*, *Physical Review D* **76** (Aug., 2007) 043517, [[astro-ph/0703757](#)].
- [38] M. Fornasa and G. Bertone, *Black Holes as Dark Matter Annihilation Boosters*, *International Journal of Modern Physics D* **17** (Jan., 2008) 1125–1157, [[0711.3148](#)].
- [39] F. Aharonian, A. G. Akhperjanian, U. B. de Almeida, A. R. Bazer-Bachi, B. Behera, M. Beilicke et al., *Search for gamma rays from dark matter annihilations around intermediate mass black holes with the HESS experiment*, *Physical Review D* **78** (Oct., 2008) 072008, [[0806.2981](#)].
- [40] M. Taoso, S. Ando, G. Bertone and S. Profumo, *Angular correlations in the cosmic gamma-ray background from dark matter annihilation around intermediate-mass black holes*, *Physical Review D* **79** (Feb., 2009) 043521, [[0811.4493](#)].
- [41] T. Bringmann, J. Lavalle and P. Salati, *Intermediate Mass Black Holes and Nearby Dark Matter Point Sources: A Critical Reassessment*, *Physical Review Letters* **103** (Oct., 2009) 161301, [[0902.3665](#)].

- [42] G. Bertone, M. Fornasa, M. Taoso and A. R. Zentner, *Dark matter annihilation around intermediate mass black holes: an update*, *New Journal of Physics* **11** (Oct., 2009) 105016, [[0905.4736](#)].
- [43] A. X. Gonzalez-Morales, S. Profumo and F. S. Queiroz, *Effect of black holes in local dwarf spheroidal galaxies on gamma-ray constraints on dark matter annihilation*, *Physical Review D* **90** (Nov., 2014) 103508, [[1406.2424](#)].
- [44] M. Wanders, G. Bertone, M. Volonteri and C. Weniger, *No WIMP mini-spikes in dwarf spheroidal galaxies*, *J. Cosmol. Astropart. Phys.* **2015** (Apr., 2015) 004, [[1409.5797](#)].
- [45] T. Lacroix and J. Silk, *Intermediate-mass Black Holes and Dark Matter at the Galactic Center*, *Astrophys. J. Lett.* **853** (Jan., 2018) L16, [[1712.00452](#)].
- [46] J.-G. Cheng, S. Li, Y.-Y. Gan, Y.-F. Liang, R.-J. Lu and E.-W. Liang, *On the gamma-ray signals from UCMH/mini-spike accompanying the DAMPE 1.4 TeV  $e+e-$  excess*, *Monthly Notices of the Royal Astronomical Society* **497** (07, 2020) 2486–2492, [<https://academic.oup.com/mnras/article-pdf/497/2/2486/33576316/staa2092.pdf>].
- [47] E. C. F. S. Fortes, O. D. Miranda, F. W. Stecker and C. A. Wuensche, *Dark matter annihilation in the most luminous and the most massive ultra-compact dwarf galaxies (UCD)*, *J. Cosmol. Astropart. Phys.* **2021** (Mar., 2021) 003, [[2003.02383](#)].
- [48] G. Bertone, *Prospects for detecting dark matter with neutrino telescopes in intermediate mass black hole scenarios*, *Physical Review D* **73** (May, 2006) 103519, [[astro-ph/0603148](#)].
- [49] M. Cirelli, G. Corcella, A. Hektor, G. Hütsi, M. Kadastik, P. Panci et al., *PPPC 4 DM ID: a poor particle physicist cookbook for dark matter indirect detection*, *J. Cosmol. Astropart. Phys.* **2011** (Mar., 2011) 051, [[1012.4515](#)].
- [50] J. F. Navarro, C. S. Frenk and S. D. M. White, *The Structure of Cold Dark Matter Halos*, *Astrophysical Journal* **462** (May, 1996) 563, [[astro-ph/9508025](#)].
- [51] J. F. Navarro, C. S. Frenk and S. D. M. White, *A Universal Density Profile from Hierarchical Clustering*, *Astrophysical Journal* **490** (Dec., 1997) 493–508, [[astro-ph/9611107](#)].
- [52] A. Tamm, E. Tempel, P. Tenjes, O. Tihhonova and T. Tuvikene, *Stellar mass map and dark matter distribution in M 31*, *Astron. Astrophys* **546** (Oct., 2012) A4, [[1208.5712](#)].
- [53] P. Gondolo and J. Silk, *Dark Matter Annihilation at the Galactic Center*, *Physical Review Letters* **83** (Aug., 1999) 1719–1722, [[astro-ph/9906391](#)].
- [54] P. J. E. Peebles, *Star Distribution Near a Collapsed Object*, *Astrophysical Journal* **178** (Dec., 1972) 371–376.
- [55] S. Tremaine, K. Gebhardt, R. Bender, G. Bower, A. Dressler, S. M. Faber et al., *The Slope of the Black Hole Mass versus Velocity Dispersion Correlation*, *Astrophysical Journal* **574** (Aug., 2002) 740–753, [[astro-ph/0203468](#)].
- [56] T. Lacroix, C. BÅ‘hm and J. Silk, *Probing a dark matter density spike at the Galactic Center*, *Physical Review D* **89** (Mar., 2014) 063534, [[1311.0139](#)].
- [57] R. Schneider, A. Ferrara, B. Ciardi, V. Ferrari and S. Matarrese, *Gravitational wave signals from the collapse of the first stars*, *Mon. Not. R. Astron. Soc.* **317** (Sept., 2000) 385–390, [[astro-ph/9909419](#)].
- [58] C. L. Fryer, S. E. Woosley and A. Heger, *Pair-Instability Supernovae, Gravity Waves, and Gamma-Ray Transients*, *Astrophysical Journal* **550** (Mar., 2001) 372–382, [[astro-ph/0007176](#)].
- [59] A. Heger, C. L. Fryer, S. E. Woosley, N. Langer and D. H. Hartmann, *How Massive Single Stars End Their Life*, *Astrophysical Journal* **591** (July, 2003) 288–300, [[astro-ph/0212469](#)].
- [60] P. Marigo, C. Chiosi and R. P. Kudritzki, *Zero-metallicity stars. II. Evolution of very massive objects with mass loss*, *Astron. Astrophys* **399** (Feb., 2003) 617–630, [[astro-ph/0212057](#)].

- [61] P. Madau and M. J. Rees, *Massive Black Holes as Population III Remnants*, *Astrophys. J. Lett.* **551** (Apr., 2001) L27–L30, [[astro-ph/0101223](#)].
- [62] O. Y. Gnedin, *Million solar mass black holes at high redshift*, *Classical and Quantum Gravity* **18** (Oct., 2001) 3983–3988, [[astro-ph/0108070](#)].
- [63] V. Bromm and A. Loeb, *Formation of the First Supermassive Black Holes*, *Astrophysical Journal* **596** (Oct., 2003) 34–46, [[astro-ph/0212400](#)].
- [64] S. M. Koushiappas, J. S. Bullock and A. Dekel, *Massive black hole seeds from low angular momentum material*, *Mon. Not. R. Astron. Soc.* **354** (Oct., 2004) 292–304, [[astro-ph/0311487](#)].
- [65] S. Abdollahi, F. Acero, M. Ackermann, M. Ajello, W. B. Atwood, M. Axelsson et al., *Fermi Large Area Telescope Fourth Source Catalog*, *Astrophys. J. Suppl.* **247** (Mar., 2020) 33, [[1902.10045](#)].
- [66] T. Isobe, E. D. Feigelson and P. I. Nelson, *Statistical Methods for Astronomical Data with Upper Limits. II. Correlation and Regression*, *Astrophysical Journal* **306** (July, 1986) 490.
- [67] J. Lyu, G. H. Rieke and S. Alberts, *The Contribution of Host Galaxies to the Infrared Energy Output of  $z \gtrsim 5.0$  Quasars*, *Astrophysical Journal* **816** (Jan., 2016) 85, [[1511.05938](#)].
- [68] M. Abdughani, Y.-Z. Fan, L. Feng, Y.-L. Sming Tsai, L. Wu and Q. Yuan, *A common origin of muon  $g-2$  anomaly, Galaxy Center GeV excess and AMS-02 anti-proton excess in the NMSSM*, *arXiv e-prints* (Apr., 2021) arXiv:2104.03274, [[2104.03274](#)].
- [69] B. Abi, T. Albahri, S. Al-Kilani, D. Allspach, L. P. Alonzi, A. Anastasi et al., *Measurement of the Positive Muon Anomalous Magnetic Moment to 0.46 ppm*, *Physical Review Letters* **126** (Apr., 2021) 141801, [[2104.03281](#)].
- [70] M.-Y. Cui, Q. Yuan, Y.-L. S. Tsai and Y.-Z. Fan, *Possible Dark Matter Annihilation Signal in the AMS-02 Antiproton Data*, *Physical Review Letters* **118** (May, 2017) 191101, [[1610.03840](#)].
- [71] A. Cuoco, M. Krämer and M. Korsmeier, *Novel Dark Matter Constraints from Antiprotons in Light of AMS-02*, *Physical Review Letters* **118** (May, 2017) 191102, [[1610.03071](#)].
- [72] J. S. Bullock, A. Dekel, T. S. Kolatt, A. V. Kravtsov, A. A. Klypin, C. Porciani et al., *A Universal Angular Momentum Profile for Galactic Halos*, *Astrophysical Journal* **555** (July, 2001) 240–257, [[astro-ph/0011001](#)].
- [73] A. Berlin, D. Hooper and S. D. McDermott, *Simplified dark matter models for the Galactic Center gamma-ray excess*, *Physical Review D* **89** (June, 2014) 115022, [[1404.0022](#)].
- [74] C. R. Harris, K. J. Millman, S. J. van der Walt, R. Gommers, P. Virtanen, D. Cournapeau et al., *Array programming with NumPy*, *Nature* **585** (Sept., 2020) 357–362, [[2006.10256](#)].
- [75] P. Virtanen, R. Gommers, T. E. Oliphant, M. Haberland, T. Reddy, D. Cournapeau et al., *SciPy 1.0: fundamental algorithms for scientific computing in Python*, *Nature Methods* **17** (Feb., 2020) 261–272, [[1907.10121](#)].
- [76] J. D. Hunter, *Matplotlib: A 2D Graphics Environment*, *Computing in Science and Engineering* **9** (May, 2007) 90–95.

## A: Constraints on the DM parameters

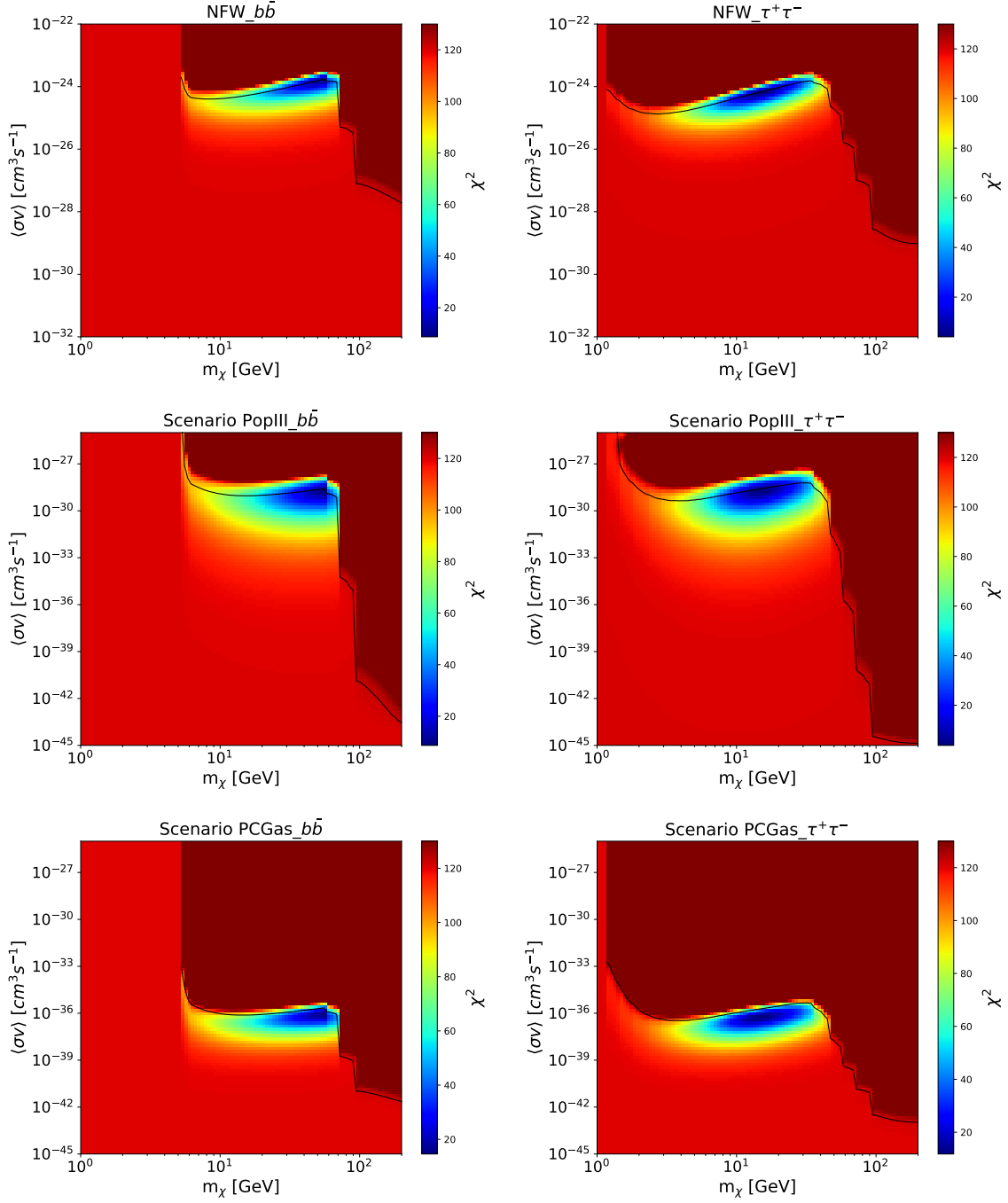


**Figure 3:** The  $\chi^2$  value as a function of the DM mass  $m_\chi$  and annihilation cross section  $\langle\sigma v\rangle$  for three models (*NFW*, *Scenario PopIII* and *Scenario PCGas*) with the  $b\bar{b}$  and  $\tau^+\tau^-$  channels, separately. The black lines are the 95% confidence level upper limits of  $\langle\sigma v\rangle$ .